Environmental Chemistry and Ecotoxicology 1 (2019) 26–35

Contents lists available at ScienceDirect

Environmental Chemistry and Ecotoxicology

journal homepage: www.keaipublishing.com/en/journals/environmental-chemistry-and-ecotoxicology/

Element analysis and bioaccessibility assessment of ultrafine airborne particulate matter ($PM_{0.1}$) using simulated lung fluid extraction (artificial lysosomal fluid and Gamble's solution)

Hanne Weggeberg *, Tonje Fagertun Benden, Eiliv Steinnes, Trond Peder Flaten

Department of Chemistry, Norwegian University of Science and Technology (NTNU), NO-7491 Trondheim, Norway

ARTICLE INFO

Article history:
Received 15 July 2019
Received in revised form 9 August 2019
Accepted 13 August 2019
Available online 15 August 2019

Keywords:
Airborne particulate matter
Trace elements
Metal bioaccessibility
Ultrafine particles
Source apportionment
Simulated lung fluids

ABSTRACT

Chemical characterization and source and bioaccessibility investigations were performed on airborne ultrafine particles (UFPs) collected from a trafficked road (Elgeseter) and a city background site (Torget) within the city of Trondheim, Norway from January 2014 to May 2015. Particles were collected using cascade impactors, and HNO_3 soluble element concentrations were determined using high-resolution inductively-coupled plasma mass spectrometry (HR-ICP-MS). Element bioaccessibility was assessed by extraction in simulated lung fluids, and possible sources were investigated using enrichment factor (EF) and principal component analysis (PCA).

UFP concentrations in air were somewhat higher at the roadside than at the city background site. Levels of total UFP and elemental components were variable, but overall low at both sites during the collection period. Concentrations of the typical crustal associated elements Al, Th, and Sc were highest in spring and summer at Elgeseter, indicating considerable contribution from re-suspension of road dust with mixed origin to atmospheric levels. W, known to be associated with studded tire wear, was highest in spring.

Source identification analysis using enrichment factors and PCA indicated direct vehicular emissions, and re-suspension of road dust largely consisting of crustal-derived materials, as the two predominant sources of UFPs. Elements clearly associated with vehicular traffic emissions included Sb, Zn, Pb, As, and Cu. Several elements seemed to originate from both vehicle emissions and crustal material.

To our knowledge no previous studies have investigated the bioaccessibility of metals in UFPs using extraction in simulated lung fluids. Our study indicated that solubility and thereby bioaccessibility is considerable for several potentially toxic elements found in UFPs, which may reach the inner lungs after inhalation. Solubility was overall highest for the elements Rb, Ni, As, Sn, Tl, and Cs. Extraction in the more acidic artificial lysosomal fluid (ALF) resulted in considerably higher element solubility compared to the neutral Gamble's solution.

Keywords:
Airborne particulate matter
Trace elements
Metal bioaccessibility
Ultrafine particles
Source apportionment
Simulated lung fluids

1. Introduction

Exposure to airborne particulate matter (APM) constitutes a major health risk, especially in urban areas, and is primarily associated with respiratory and cardiovascular mortality and diseases [1]. Particles' physicochemical behavior in the atmosphere, site and manner of deposition, and toxicity are strongly dependent on size. Ultrafine particles (UFPs), usually defined as particles with aerodynamic diameter <0.1 μm ($PM_{0.1}$) [2], may inhere considerable health risks due to their high numbers and large surface areas.

UFPs are formed to a large degree by motor vehicles and other combustion processes, giving rise to primary particles, and also by conversion of gases in the atmosphere forming secondary particles. Due to their tendency to undergo coagulation and condensation forming larger particles, UFPs are typically unstable with short half-lives [3]. Hence, UFPs are mainly associated with heavily trafficked roads, with concentrations decreasing rapidly with increasing distance from the roads [4,5].

Possible health effects of elemental constituents of $PM_{0.1}$ should be more thoroughly investigated. Several studies have linked the ultrafine particulate

* Corresponding author at: Rambøll Norge AS, Pb 9420, NO-7493 Trondheim, Norway.
E-mail addresses: hanne.weggeberg@ramboll.no, (H. Weggeberg), tonje.fagertun-benden@vetinst.no, (T.F. Benden), eiliv.steinnes@ntnu.no, (E. Steinnes), trond.p.flaten@ntnu.no. (T.P. Flaten).

Production and hosting by Elsevier on behalf of KeAi

http://dx.doi.org/10.1016/j.enceco.2019.08.001

fraction to respiratory and cardiovascular disease and mortality [6–9]. The precise mechanisms of toxicity for ultrafine APM are largely unknown. UFPs have been shown to cause airway inflammation, probably by induction of reactive oxygen species (ROS) [10]. In addition, UFPs may effectively cross over to the circulatory system and translocate to and exert toxic effects in other tissues and organs, such as the brain [11] or liver [12]. The small UFPs may also enter cells directly by crossing cellular membranes [13]. Elemental components of APM, and especially transition metals, have in several studies been found to be associated with mortality [14,15] and cardiovascular [16] and respiratory incidents and disease [17]. More studies are needed to elucidate the role of elements and other particle components and properties in $PM_{0.1}$ toxicity.

Elemental components are considered important contributors to APM toxicity, mainly due to their ability to produce ROS [18,19]. Transition metals such as Fe, V, and Cr may generate ROS through redox reactions, whereas redox inactive elements can induce ROS indirectly by disturbing metal homeostasis, i.e. by depletion of antioxidants such as glutathione [20].

Element solubility may provide useful estimates of bioaccessibility, the fraction that is accessible for uptake in cells and thereby exertion of toxicity [18,21]. Extraction in simulated lung fluids (SLFs) constitutes physiologically relevant, yet simple and inexpensive methods of assessing the bioaccessibility of APM. SLFs have been used in a few studies to assess the bioaccessibility of metallic components in urban air. For example, solubility in SLFs of platinum group elements has been investigated in road dust and milled vehicle exhaust catalysts [22] and in different size fractions of urban APM [23]. Some studies have used SLFs to assess bioaccessibility of a wider range of metals in different cities [24–27]. However, to our knowledge no studies have investigated the bioaccessibility of metals in the ultrafine size fraction of APM using extraction in SLFs.

In this study, a range of elements within the ultrafine fraction collected over a continuous period of 16 months from a roadside and an urban background site in the city of Trondheim, Norway were investigated. Potential bioaccessibility of the elemental components was assessed using the SLFs Gamble's solution and artificial lysosomal fluid (ALF), and possible sources were investigated using enrichment factors (EFs) and principal component analysis (PCA).

2. Methods

2.1. Test sites, and collection and preparation of UFP samples

UFP samples were collected from two municipal measurement stations within the city of Trondheim: Elgeseter station is located alongside the heavily trafficked Elgeseter main road, with annual average daily traffic (AADT) of 22,000, whereas Torget is a city background station dominated by bus traffic and domestic wood stove heating emissions, located on the roof of Torget shopping mall in the city center, 15 m above street level. Most road segments in the immediate vicinity of Torget station have AADT numbers <7000.

Samples were collected at Elgeseter and Torget stations from January 2014 to May 2015, during 32 separate time periods, yielding a total of 64 UFP samples. Sampling times varied from 144 to 216 h. Due to the long sampling times, weather conditions during most samplings were quite variable, typically including both periods with clear conditions and precipitation, and varying temperatures. The sampling was conducted using cascade impactors (Moudi model 100-S4 Special from MSP/Copley Scientific), with accompanying pressure gauges and flowmeters (model DFM2000, Copley Scientific) or membrane pumps with flow rate 30 ± 1 L/min. TSP inlets with 1 m long tubes (Digitel) were used. Zefluor PTFE filters with pore size 2.0 μm and diameter 47 mm (VWR) were used.

The filters were weighed, stored and placed into the impactors in an ISO 6 cleanroom, and handled with plastic tweezers. All equipment used in the treatment of the filters was cleaned with ultrapure nitric acid (HNO_3, 0.1 M). The impactor nozzle plate was soaked in methanol overnight after each collection. Field blank samples consisted of filters that were conditioned, weighed, stored, transported to the test site, and assembled in the sampling equipment in the same manner as the sample filters, apart from applying flow and thereby APM collection. The certified standard reference materials (SRMs) used were Urban Particulate Matter 1648a (NIST), Urban Aerosols No. 28 (NIES), and INCT-PVTL-6 Polish Virginia Tobacco Leaves (ICHTJ).

Particle mass on the filters was weighed based on the method described in European Standard EN 12341:2014 [28]. The filters were conditioned in desiccators placed in plastic petri dishes with the lids ajar and weighed before and after particle loading. Conditioning time was 48 h before the first, and 24 h before the second weighing. If the parallel masses differed by >0.5 mg, another weighing was performed after 24 h. Samples were weighed with a 5-decimal microbalance (Sartorius). Accuracy and drift of the balance were checked with a 200-mg reference mass and a blank reference filter. The unloaded and loaded filters were stored in the cleanroom until assembly in the impactors and GMB extraction, respectively. Further details regarding the test sites and the collection and preparation of UFP samples are given in an online supplementary file, and in an upcoming article, where a small subset of the samples analyzed in this work was used.

2.2. Preparation of simulated lung fluids and extraction procedure

Element bioaccessibility was investigated using two different simulated lung fluids (SLFs): Gamble's solution and artificial lysosomal fluid (ALF). Gamble's solution contains inorganic salts and organic acids and simulates the interstitial lung fluid found within the deep lung, whereas the composition of ALF represents the acidic intracellular conditions in lung cells caused by phagocytosis under stressed conditions [29–31]. The SLFs were prepared according to the procedure used by Herting et al. [29]. Chemicals used were of analytical grade, and ultrapure water was used throughout (Purelab Option-Q7, Elga, UK). All equipment used in SLF preparation and extraction was cleaned with HNO_3 (0.1 M) and rinsed with ultrapure water. SLFs were prepared in Teflon bottles and the samples extracted in a laminar air flow (LAF) bench. The pH was adjusted to 7.4 using NaOH (50%) and HCl (25%). Loaded filters were cut in two with steel scissors or a scalpel, resulting in filter pieces containing on average 0.5 mg dust, and placed in polyethylene vessels (15 mL). SLF (5 mL) was added, and the vessels were placed in an incubator and subjected to bilinear shaking (125 cycles/min, 37 °C, 24 h). pH was determined in selected samples after extraction to check pH stability. After extraction the filters were removed and placed in new sets of polyethylene vessels, whereas the solutions were centrifuged (10 min., 710 relative centrifugal force (rcf)) prior to ICP-MS analysis. Blank and SRM samples were extracted following the same procedure as the dust filters.

2.3. Determination of elements using ICP-MS

The supernatant was decanted into new sets of polyethylene vessels, acidified with concentrated HNO_3 and diluted with ultrapure water to a final HNO_3 concentration of 0.6 M prior to ICP-MS analysis. Precipitate samples were transferred to Teflon UltraClave vessels (18 mL) with ultrapure HNO_3 (50% v/v, two times 1 mL), and dissolved together with the filters using an UltraClave microwave-assisted autoclave (Milestone) with a gradual rise to 245 °C and 160 bar. Subsequently, the samples were diluted to 0.6 M HNO_3 and transferred to new polyethylene tubes and stored at room temperature until ICP-MS analysis.

Element concentrations were determined using high-resolution inductively-coupled plasma mass spectrometry (HR-ICP-MS, Element 2, Thermo Finnigan) using an SC-FAST flow injection system for SC-4 (ESI). Three different resolutions were applied to avoid interferences: low (400), medium (5000) and high (10000). Detection limits were set to three times the standard deviations of element concentrations in blank samples.

2.4. Statistical analysis

Element concentration differences between test sites were investigated using the nonparametric Mann-Whitney *U* test. Seasonal differences were analyzed using the Kruskal-Wallis H test with Dunn post hoc testing. Element concentrations below the limit of detection (LOD) were imputed according to Flynn (2010) [32], by constrained maximization of the Shapiro-Wilk *W* statistic assuming lognormal distribution.

Enrichment factors (EFs) were used as initial indicators of the degree of anthropogenic contribution to the element levels determined in the $PM_{0.1}$ samples [33], and were calculated according to the following formula:

$$EF_X = \left([X]_{sample}/[Al]_{sample}\right)/\left([X]_{crust}/[Al]_{crust}\right)$$

where X is the element under consideration. Al was used as reference element, and the average crustal concentrations ($[X]_{crust}$) were taken from Mason and Moore [34].

PCA with Varimax rotation and Kaiser normalization was used to examine correlations between HNO_3 soluble elemental levels relative to dust concentrations. Element concentration data was centered and scaled. Kaiser-Meyer-Olkin Measure of Sampling Adequacy (KMO), Bartlett's Test of Sphericity (Bartlett's test), and split-sample validation were used to assess validity of the PCA model. Variables for which Pearson correlation coefficients for replicate samples (filter halves that underwent the same treatment) after SLF extraction were below 0.7 were excluded from EF, PCA and bioaccessibility analysis. Statistical treatment was conducted with SPSS 22.0 (IBM) and R 3.2.0 (CRAN).

3. Results and discussion

3.1. Levels of airborne ultrafine particles (UFP)

Concentrations of UFP and element components of UFP are presented in Table 1. Total UFP levels were variable but overall low, and somewhat higher at Elgeseter than at Torget; medians 1.4 μg/m^3 and 0.97 μg/m^3, $p = 0.048$. Levels ranged from less than detectable to 8.1 and 5.3 μg/m^3 at Elgeseter and Torget, respectively. Median $PM_{0.1}$ levels were lower than the means, showing that the distributions of the data were right-skewed.

Urban UFP air concentrations vary considerably between different sites. Pakkanen et al. [35] found a lower mean $PM_{0.1}$ concentration (0.49 μg/m^3) in Helsinki, Finland than in the present study. Mean $PM_{0.1}$ mass concentrations found in this study were comparable to those reported by Gugamsetty et al. [36] of 1.42 ± 0.56 μg/m^3 for a trafficked area in New Taipei City, Taiwan, whereas Lin et al. [37] obtained mean $PM_{0.1}$ concentrations as high as 54 μg/m^3 near a heavily trafficked road in Southern Taiwan. No regulatory limit values exist for the ultrafine APM fraction. In Erfurt, Germany, Airborne UFPs were found to be associated with increased respiratory and cardiovascular mortality, independently of fine particles ($PM_{2.5}$), at a mean mass concentration of 0.64 μg/m^3 [9], which is lower than in the present study. Previous studies have found associations between $PM_{0.1}$ particle number and respiratory symptoms in adult asthmatics [7], cardiac stress in patients with coronary heart disease [6], and mortality [8], at particle number concentrations comparable to those determined in the Erfurt study referred to above [9]. Number concentrations found in these studies cannot be compared to the mass concentrations found in our study, but taken together these results may indicate that the $PM_{0.1}$ levels in Trondheim could contribute to adverse health effects.

3.2. Analytical considerations

Low $PM_{0.1}$ levels complicated our ICP-MS analyses; for some of the elements, considerable proportions of samples were below the LODs. Low UFP masses on the filters (on average the filter pieces contained only about 0.5 mg dust) imply considerable uncertainties in the weighing and thereby the calculated $PM_{0.1}$ and element atmospheric mass concentrations. Accuracy and reproducibility were investigated using standard reference materials (SRM) and replicate sample analysis; methodology and results for the quality control are described in detail in an upcoming article and in the online supplementary material. Recoveries obtained for the SRM samples were overall relatively constant. Eight out of 10 elements had recoveries between 80 and 120% for Urban Aerosols UA No. 28 (NIES), and for 9 out of the 10 elements the 95% confidence intervals for the certified concentrations and our analytical results overlap. For Soil GBW 07408, 13

Table 1
Total mass of ultrafine particulate matter ($PM_{0.1}$) and element concentrations (in pg/m^3, unless otherwise stated) in road traffic (Elgeseter) and city background (Torget) samples ($N = 32$ from both sampling stations), collected between January 2014 and May 2015.

	Elgeseter				Torget				Median ratio	*p*-Value	LOD	<LOD
	Median	Mean	SD	Range	Median	Mean	SD	Range				
$PM_{0.1}$ (□g/m^3)	1.4	1.7	1.4	<0.01–8.1	0.97	1.2	0.9	<0.01–5.3	1.4	**0.048**	0.01	2
Al (ng/m^3)	13	18	16	1.1–70	12	17	14	1.0–65	1.1	0.94	0.2	0
As	34	58	68	5.5–330	34	48	43	11–210	1.0	0.97	2	0
Cd	5.2	7.0	7.4	0.68–39	4.9	7.6	6.7	1.5–33	1.1	0.52	0.2	0
Ce	21	23	15	<4–71	14	18	12	<4–46	1.5	0.26	4	6
Co	10	13	10	1.9–44	7.5	10	7.7	3.4–37	1.4	0.41	0.6	0
Cr	110	150	100	<30–380	70	76	46	<30–200	1.6	***0.003***	30	7
Cs	0.90	1.3	1.3	0.13–6.8	0.94	1.4	2.0	0.29–12	1.0	0.95	0.04	0
Cu (ng/m^3)	0.71	0.83	0.51	0.047–2.3	0.39	0.47	0.46	0.16–2.7	1.8	***<0.001***	0.02	0
Fe (ng/m^3)	20	28	22	0.66–87	14	20	14	5.3–67	1.5	0.07	0.3	0
Mn (ng/m^3)	0.30	0.42	0.31	0.068–1.3	0.28	0.35	0.24	0.11–1.2	1.1	0.53	0.003	0
Ni	48	78	76	15–370	47	65	85	12–510	1.0	0.31	10	0
Pb	110	190	220	<30–990	100	140	120	<30–580	1.1	0.75	30	5
Pt	<1	<1	0.34	<1–1.2	<1	<1	0.72	<1–4.0		0.59	1	58
Rb	31	35	22	7.8–81	29	33	19	7.7–79	1.1	0.86	1	0
Sb	90	119	92	13–420	49	65	54	13–280	1.8	***0.002***	0.4	0
Sc	3.3	5.1	4.9	0.13–20	3.0	4.4	4.0	0.29–20	1.1	0.77	0.1	0
Sn (ng/m^3)	0.13	0.26	0.41	<0.06–2.1	0.066	0.27	0.49	<0.06–2.2	1.9	0.15	0.06	20
Sr (ng/m^3)	0.26	0.32	0.23	<0.1–1.1	0.22	0.25	0.16	<0.1–0.75	1.2	0.25	0.1	4
Th	1.4	1.7	1.4	0.10–6.0	1.1	1.4	0.92	0.19–3.7	1.3	0.61	0.07	0
Tl	0.53	0.68	0.58	0.091–2.6	0.50	0.67	0.58	0.12–3.1	1.1	0.86	0.02	0
V	46	66	54	8.2–230	51	62	53	8.1–270	0.9	0.95	0.8	0
W	8.9	14	15	0.6–61	6.7	9.4	8.8	1.0–38	1.3	0.25	0.3	0
Zn (ng/m^3)	1.4	1.5	0.91	0.22–4.2	1.0	1.2	0.71	0.33–3.7	1.4	0.15	0.2	0

SD = standard deviation; LOD = limit of detection. Differences between Elgeseter and Torget means for APM and elemental constituent concentrations were analyzed using the Mann-Whitney U test. *p*-values in bold signify statistical significance at the 0.05 level, whereas p-values in bold and italic signify statistical significance at the 0.01 level.

Table 2
$PM_{0.1}$ (□g/m^3) and element concentrations (in □g/g, unless otherwise stated) in road traffic (Elgeseter) and city background (Torget) samples, collected in winter (November–February), spring (March–April), summer (May–August), and fall (September–October) 2014/2015.

	Winter (a)				Spring (b)				Summer (c)				Fall (d)			
	Elgeseter (N = 12)		Torget (N = 13)		Elgeseter (N = 8)		Torget (N = 7)		Elgeseter (N = 5)		Torget (N = 5)		Elgeseter (N = 6)		Torget (N = 6)	
	Median	Range	Median	Range	Median	Range	Median	Range	Median	Range	Median	Range	Median	Range	Median	Range
$PM_{0.1}$	1.8	0.2–2.7	**1.5b,d**	0.8–5.3	1.3	0.7–2.9	**0.9a**	0.4–1.2	1.6	0.5–2.2	0.9	0.5–1.3	1.3	0.6–8.1	**0.8a**	0.4–1.3
Al (mg/g)	**5.7b**	0.6–38	10	0.9–20	**16a**	9.6–32	15	6.7–30	22	9.0–31	10	5.8–16	8.4	1.2–19	16	7.5–33
As	**46b**	5.9–140	52	7.3–100	**20a**	7.7–32	**24d**	12–50	22	10–48	27	19–20	43	3.2–47	**68b**	41–74
Ce	13	< 3–84	17	8.4–32	18	3.8–26	15	4.4–26	18	12–30	14	6.9–18	15	< 3–32	16	7.9–19
Co	4.4	1.0–30	7.0	3.5–14	10	5.8–19	10	4.2–17	12	6.5–19	8.7	4.2–10	6.5	1.0–14	8.5	4.9–11
Cr	69	< 30–420	69	< 30–95	99	54–130	72	< 30–100	110	68–190	54	< 30–99	110	36–440	77	59–130
Cs	0.68	0.12–1.4	0.97	0.4–1.3	0.75	0.36–1.4	0.97	0.5–1.9	0.92	0.61–1.3	0.71	0.61–0.75	0.72	0.07–7.8	0.93	0.52–13
Cu (mg/g)	0.51	0.02–3.2	0.36	0.07–1.0	0.42	0.31–0.74	0.24	0.18–0.48	0.56	0.32–1.3	0.34	0.23–0.42	0.68	0.11–1.7	0.39	0.34–0.71
Fe (mg/g)	11	0.3–65	16	5.2–24	20	13–44	14	7.8–32	26	12–42	14	8.0–20	17	2.3–35	16	8.0–20
Mn (mg/g)	0.22	0.04–1.0	0.26	0.11–0.46	0.30	0.17–0.57	0.26	0.14–0.47	0.40	0.22–0.62	0.22	0.15–0.30	0.23	0.03–0.52	0.30	0.24–0.48
Ni	30	9.5–160	45	21–95	44	24–250	53	27–150	53	31–110	44	16–44	38	14–300	47	33–97
Pb (mg/g)	0.10	< 0.03–0.40	0.11	0.05–0.26	0.081	< 0.03–0.16	0.13	0.04–0.15	0.080	0.04–0.14	**0.077d**	0.05–0.077	0.085	< 0.03–1.1	**0.15c**	0.10–0.21
Pt	< 1	< 1–1.0	< 1	< 1–2.7	< 1	< 1	< 1	< 1–2.3	< 1	< 1–2.0	< 1	< 1	< 1	< 1	< 1	< 1–1.4
Rb	27	7.7–110	36	12–56	25	13–36	27	17–60	22	14–35	23	11–25	17	2.4–31	27	8.6–70
Sb	73	6.6–370	54	9.5–140	52	27–130	38	15–65	85	46–230	45	40–52	96	10–170	67	33–94
Sc	**1.3b,c**	0.1–8.1	3.2	0.3–6.2	**4.7a**	2.4–8.5	3.8	2.9–8.5	**6.4a**	2.5–9.3	2.8	1.5–4.7	2.3	0.3–6.4	3.0	1.7–4.7
Sn (mg/g)	0.062	< 0.06–0.60	< 0.06	< 0.06–0.39	0.095	< 0.06–0.22	0.14	< 0.06–1.1	< 0.06	< 0.06–0.42	< 0.06	< 0.06–0.095	0.17	0.09–0.70	0.21	< 0.06–3.5
Sr (mg/g)	0.19	< 0.1–1.2	0.12	< 0.1–0.89	0.20	0.14–0.44	0.25	< 0.1–0.91	0.16	< 0.1–0.49	0.26	0.13–0.20	0.17	< 0.1–0.39	0.22	0.11–1.5
Th	**0.43b,c**	0.07–4.6	0.88	0.18–1.8	**1.6a**	0.9–2.7	1.4	0.8–2.3	**2.0a**	1.2–2.6	1.1	0.6–1.6	0.73	0.12–2.0	1.3	0.5–1.5
Tl	0.47	0.14–3.1	0.61	0.25–1.2	0.32	0.17–1.8	0.41	0.29–1.0	0.32	0.16–0.74	0.40	0.17–0.32	0.35	0.04–0.51	0.49	0.27–0.72
V	**17c**	6.3–130	38	7.9–63	52	34–95	63	37–110	**87a**	60–110	73	39–52	36	4.6–73	48	38–67
W	5.9	0.5–24	7.9	1.5–15	**14d**	9.0–40	**13d**	3.7–23	7.5	2.3–12	2.4	1.7–14	**3.6a**	0.5–8.3	**2.9b**	0.9–11
Zn (mg/g)	0.97	0.2–2.8	1.3	0.3–1.8	0.79	0.39–2.2	0.91	0.37–2.3	0.95	0.71–1.7	0.84	0.57–0.79	1.0	0.1–2.2	1.3	1.0–2.0

Differences between means for the different seasons were analyzed with the Kruskal-Wallis H test and Dunn post hoc test. Seasonal means that differ from other means statistically at the 0.05 level are marked in bold, with the group (s) they differ from specified (a = winter, b = spring, c = summer, and d = fall). Elgeseter and Torget samples were analyzed separately.

Table 3
Enrichment factors (EFs) in road traffic (Elgeseter) and city background (Torget) ultrafine particulate matter samples, collected between January 2014 and May 2015.

	Winter				Spring				Summer				Fall			
	Elgeseter (N = 12)		Torget (N = 12)		Elgeseter (N = 8)		Torget (N = 8)		Elgeseter (N = 5)		Torget (N = 5)		Elgeseter (N = 7)		Torget (N = 7)	
	Mean	SD	Mean	SD	Mean	SD	Mean	SD	Mean	SD	Mean	SD	Mean	SD	Mean	SD
Al	1		1		1		1		1		1		1		1	
As	620	600	440	610	50	19	84	73	67	45	100	56	180	64	200	100
Ce	5.3	6.3	3.5	3.5	1.2	0.5	1.1	0.5	1.5	0.3	1.6	0.3	2.1	0.9	1.6	0.9
Co	3.9	2.2	3.2	2.9	2.1	0.2	2.0	0.3	2.2	0.3	2.2	0.4	2.7	0.4	2.0	0.9
Cr	15	14	6.5	3.7	4.5	1.8	3.3	1.7	5.6	1.2	3.5	1.0	13.6	9.4	4.4	2.1
Cs	4.4	4.6	4.4	5.6	1.3	0.4	1.5	0.5	1.5	0.9	1.9	0.9	3.7	4.5	6.5	12.7
Cu	190	160	87	93	41	11	25	8.1	56	25	160	270	140	63	52	27
Fe	4.6	3.6	3.1	2.0	2.1	0.2	1.7	0.3	2.4	0.6	2.0	0.2	3.4	0.8	1.9	0.9
Mn	3.8	2.3	3.1	2.2	1.6	0.1	1.5	0.3	1.9	0.3	1.9	0.2	2.5	0.4	2.0	0.8
Ni	12	14	6.7	6.2	4.0	2.5	4.6	3.0	4.2	3.4	3.2	1.8	11.2	9.7	4.1	1.9
Pb	190	180	130	150	40	31	43	24	38	35	42	25	150	160	70	46
Rb	7.7	7.5	6.2	8.6	1.4	0.7	1.5	0.5	1.1	0.2	1.8	1.1	2.1	0.9	2.3	1.7
Sb	7200	5300	3900	4200	1400	290	910	300	2400	1500	2000	1300	4500	1800	2100	1100
Sc	1.2	1.3	1.0	0.2	1.0	0.1	1.0	0.3	1.1	0.1	1.0	0.1	1.1	0.2	0.8	0.4
Sn	810	600	760	1100	270	280	470	560	270	290	390	530	8200	17,000	1300	1600
Sr	20	26	8.6	16	3.6	2.9	5.0	4.9	2.6	1.6	3.9	1.6	9.5	10.7	7.5	7.0
Th	1.1	0.5	1.1	0.4	1.3	0.8	1.0	0.5	1.1	0.2	1.1	0.2	1.1	0.2	0.9	0.5
Tl	28	28	19	29	4.6	4.8	6.2	4.3	4.2	5.1	5.6	5.1	6.0	2.5	7.9	6.2
V	2.8	1.6	2.3	1.0	2.0	0.3	2.2	0.6	3.0	1.2	4.6	4.1	2.5	0.5	2.2	1.2
W	69	38	44	18	52	9.1	39	10	19	7.1	17	5.5	22	6.9	15	13
Zn	340	390	280	440	83	81	69	44	73	30	78	40	150	62	110	52

out of 19 elements had recoveries between 80 and 100%, but recoveries were low for some of the elements. This is most probably because our HNO_3/Ultraclave digestion procedure does not completely dissolve all siliceous minerals. Thus, for some of the elements, the concentrations found are most likely somewhat underestimated compared to total element contents.

Contamination on the collection filters by larger particles could potentially affect the concentrations. We investigated some of the filters qualitatively by scanning electron microscopy (SEM); example SEM images of the sampled UFP fraction are shown in an online Supplementary material. Very few larger particles were seen, but these could nevertheless cause significant overestimation of $PM_{0.1}$ and element mass concentrations.

Table 4
Principal component analysis (PCA) variable loadings and communalities, and percent variance explained for each principal component (PC), for airborne ultrafine particulate matter ($PM_{0.1}$) and elemental constituent levels.

	PC1	PC2	Com.
	37%	24%	
Al	**0.90**	0.08	0.82
As	−0.14	**0.74**	0.57
Ce	**0.67**	**0.56**	0.76
Co	**0.95**	0.23	0.96
Cr	**0.56**	**0.58**	0.65
Cs	0.09	0.27	*0.08*
Cu	0.25	**0.58**	*0.40*
Fe	**0.89**	0.37	0.93
Mn	**0.89**	0.38	0.94
Ni	**0.54**	0.31	*0.39*
Pb	0.07	**0.64**	*0.41*
Rb	0.09	**0.68**	*0.47*
Sb	**0.45**	**0.73**	0.74
Sc	**0.95**	−0.05	0.91
Sn	0.04	0.28	*0.08*
Sr	0.00	**0.49**	*0.24*
Th	**0.91**	0.18	0.86
Tl	0.31	**0.64**	0.51
V	**0.79**	0.00	0.62
W	**0.76**	−0.01	0.58
Zn	0.17	**0.85**	0.75

Loadings larger than 0.4 are shown in bold, and communalities lower than 0.5 in italic.

3.3. UFP elemental contents

Element concentrations in the ultrafine fraction were variable, but generally low for most elements (Table 1); Pt, Tl, Cs, Th, Sc, Co, W, Ce, Rb, As, V, Ni, Sb, and Cr, ordered from lowest to highest, all occurred at pg/m^3 levels. The major crustal elements Fe and Al exhibited the highest air concentrations. Traffic-related elements such as Cu, Sn, Pb, Cr, Sb, Ni, V, and As occurred at lower concentrations. Concentrations of most elements were generally somewhat higher at Elgeseter station, except for Cd and Cs which were slightly higher at Torget, although most of these differences were not statistically significant. Differences were largest for Cu, Sb, and Cr, which had median levels between 1.6 and 1.8 times higher for Elgeseter compared to Torget samples, and these five differences were all statistically significant at the 0.01 level. Element air concentrations in this study were generally comparable to those found by Pakkanen et al. [35], while Gugamsetty et al. [36] reported overall somewhat lower element concentrations. Lin et al. [37], on the other hand, reported overall considerably higher element air concentrations.

3.4. Seasonal differences

Total UFP concentrations in air were overall highest in winter (November–February), at both Torget and Elgeseter stations, but significant differences were only found for Torget (Table 2). Indeed, particulate matter levels are expected to be higher in winter, due to increased motor vehicle traffic, domestic wood burning and occurrence of atmospheric inversions [38]. In the studied area, airborne particulate matter concentrations might also be expected to increase during periods in spring (March–April) due to re-suspension of sand and road salt applied to the roads in winter. In October particulate matter levels may increase when vehicles change to studded tires before snow has fallen. One reason why the observed seasonal variations were not as pronounced as might have been expected, is probably the exceptionally mild winters with more precipitation than normal that occurred in Trondheim during the sampling period. Such mild winters would result in less emissions and re-suspension from motor vehicles and domestic stove heating,

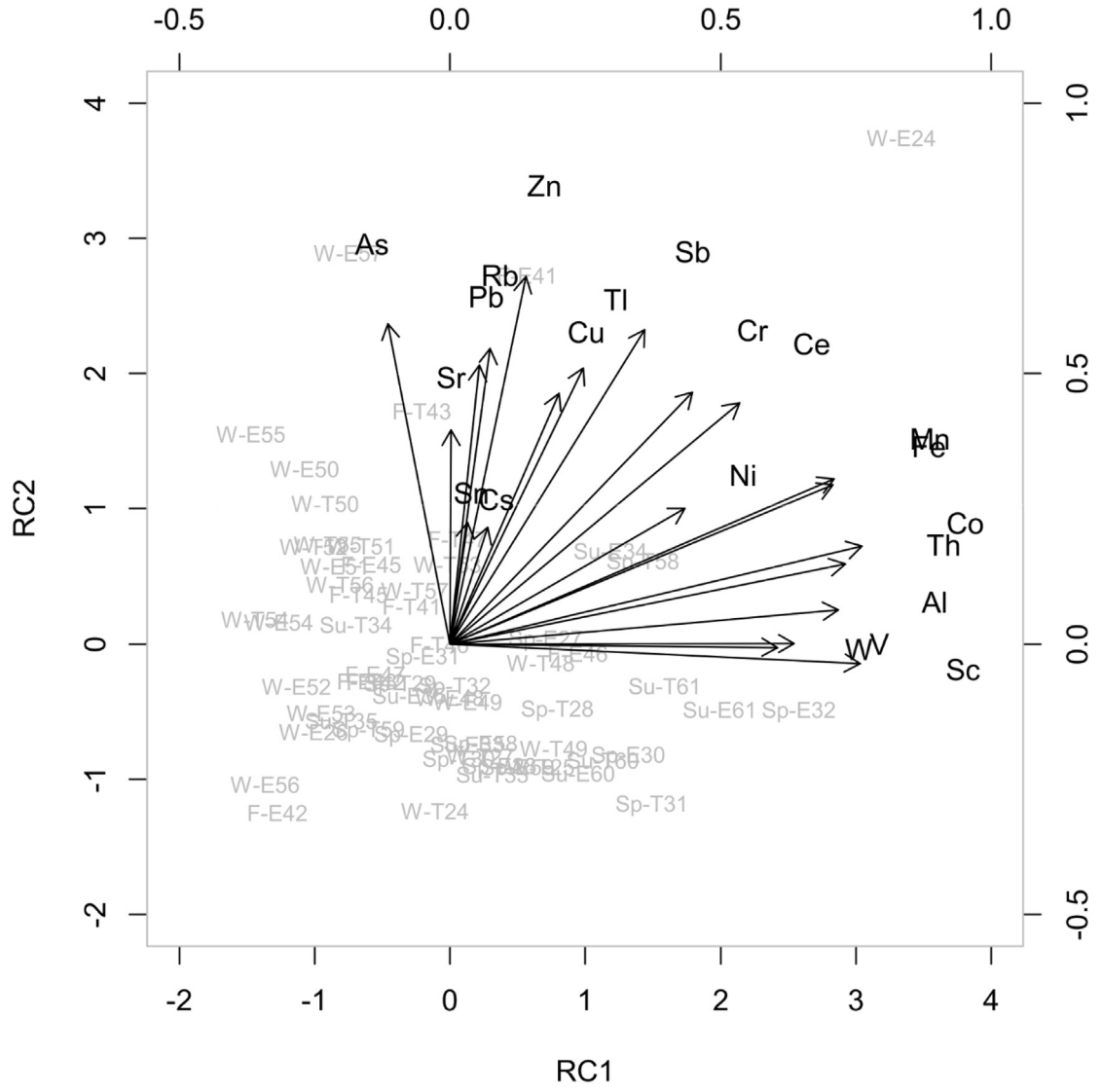

Fig. 1. Principal component (PCA) biplot, showing PCA variable loadings (upper and right axes, black arrows and variable names) and scores (lower and left axes, gray sample names; W = winter, Sp = spring, Su = summer, F = fall) for principal components (PCs) 1 and 2 for airborne ultrafine particles ($PM_{0.1}$) and elemental component levels.

and faster deposition and less re-suspension of dust. In addition, more efficient dust reduction measures were instigated during this period, involving frequent mechanical street sweeping and dust collection, and application of $MgCl_2$ salt to maintain wet roads.

Seasonal patterns in levels of airborne elemental components were not consistent, but concentrations of elements likely to be associated with geogenic material (Al, Sc, and Th) were higher in spring and summer at Elgeseter roadside station (Table 2). Concentrations of some elements, namely Al, Sc, Th, and W, were elevated during spring, and Sc, Th, and V during summer sampling periods at Elgeseter ($p < 0.05$). As concentrations were highest in winter Elgeseter samples, also statistically significant. In Torget samples, As and Pb concentrations were significantly higher during fall. Levels of W were clearly highest during spring at both sites($p < 0.05$). Patterns of seasonal differences for the remaining elements were not consistent during the sampling period.

3.5. Source analysis (EFs and PCA)

Enrichment factor (EF) analysis is commonly used as indicator of anthropogenic contribution to elemental contents in different matrices. Elements with EF values close to unity are assumed to be of predominantly crustal origin, whereas values above 10 imply considerable contribution from anthropogenic sources [39]. In this study, EFs for the UFP samples were calculated using Al as the reference element for crustal material. For most of the determined elements, EFs were clearly highest in winter; for instance, mean EFs for As for Elgeseter samples were 620 in winter, compared to 170 in fall, 67 in summer, and 50 in spring (Table 3).

Our EF analysis indicates with a high degree of certainty that Sb, Sn, As, Zn, Pb, and Cu, and most probably W and Tl, originate almost exclusively from anthropogenic sources. Most of these elements are typically associated with traffic pollution [40], emission from motor vehicles being the most likely source. The remaining reported elements seem to have soil dust as a major source, although Sr and typical traffic-related elements such as Ni and Cr had mean EFs close to 10 for Elgeseter samples, thus probably having traffic emissions as a major source. Sb clearly showed the overall highest mean EFs: Mean EFs for Sb in the winter samples were 7200 at Elgeseter and 3900 at Torget. High EF values for Sb is consistent with a study recently conducted on road dust in Trondheim, Norway [41]. EFs for most elements studied were highly variable, as shown by the high standard deviations. We cannot explain the high EFs for Sn found in fall samples. EF values found in this study are comparable to those obtained by Gugamsetty et al. [36]. EFs were generally higher at the trafficked Elgeseter station compared to Torget, which is located high above the ground. However, interpreting EF values in terms of anthropogenic contribution must be

Table 5
Element solubility (%) following extraction in Gamble's solution (GMB) and artificial lysosomal fluid (ALF) for $PM_{0.1}$.

	GMB										ALF									
	Elgeseter					Torget					Elgeseter					Torget				
	N	Median	Mean	SD	Range	N	Median	Mean	SD	Range	N	Median	Mean	SD	Range	N	Median	Mean	SD	Range
Al	25	2.6	2.7	1.3	0.9–6.4	29	3.0	3.2	1.9	0.4–7.9	19	10	10	4.3	3.5–18	16	13	13	7.6	6.0–38
As	34	59	57	16	10–80	35	65	63	12	37–86	18	66	64	14	18–81	16	65	66	11	50–84
Ce	9	4.1	17	32	1.9–100	5	4.0	4.3	1.3	2.4–5.6	–	–	–	–	–	–	–	–	–	–
Co	23	15	15	4.1	7.8–23	26	19	19	7.3	5.6–37	18	41	41	8.2	21–56	16	44	43	7.0	29–53
Cr	3	38	38	9.9	28–48	–	–	–	–	–	3	22	29	18	16–50	2	–	70	–	53–87
Cs	17	48	46	18	21–86	22	52	50	18	15–90	3	48	46	17	29–63	2	–	72	–	65–78
Cu	13	15	16	5.3	8.7–28	3	34	30	8.1	21–35	17	82	77	8.9	63–92	14	81	79	7.9	62–90
Fe	19	1.4	1.7	1.1	0.5–5.0	12	1.9	1.9	1.0	0.6–100	19	34	32	11	3.9–51	16	33	33	5.8	21–42
Mn	29	5.4	7.7	9.6	1.1–52	32	5.6	6.5	4.1	1.4–100	17	45	44	7.9	29–57	16	50	50	8.8	38–71
Ni	7	62	61	20	38–100	2	–	43	–	38–49	–	–	–	–	–	–	–	–	–	–
Pb	4	4.9	6.1	3.8	3.0–12	–	–	–	–	–	12	75	73	15	42–90	11	77	74	10	52–84
Rb	6	73	70	14	46–86	8	77	75	6.1	63–81	12	61	52	19	21–73	10	61	63	20	37–100
Sb	34	22	24	13	7.5–62	35	32	35	13	13–68	18	65	63	17	29–100	16	67	69	14	52–100
Sc	–	–	–	–	–	–	–	–	–	–	10	10	11	4.0	4.8–17	4	11	13	5.6	8.3–21
Sn	4	51	51	57	1.2–100	3	2.3	34	57	1.1–100	17	44	55	29	24–100	16	100	97	14	45–100
Sr	–	–	–	–	–	–	–	–	–	–	2	–	82	–	72–92	–	–	–	–	–
Th	–	–	–	–	–	–	–	–	–	–	13	35	38	12	21–59	11	46	49	10	35–66
Tl	23	49	48	16	10–73	34	54	53	12	24–77	12	51	61	20	45–100	16	59	58	10	39–74
V	34	20	23	13	6.1–52	35	22	28	16	7.9–65	18	24	23	10	5.9–41	16	38	36	11	12–59
W	27	19	20	13	4.9–67	26	15	25	23	6.5–100	16	24	31	17	13–64	11	41	47	24	22–100
Zn	2	–	32	–	30–35	–	–	–	–	–	17	79	75	7.7	62–85	14	77	77	13	42–100

done with caution; elevated EFs may be caused by local variations in soil and bedrock composition or unknown physicochemical soil or atmospheric processes [42,43].

Possible element sources were further investigated by applying PCA to element mass concentrations relative to UFP air concentrations, with Varimax rotation to maximize element variable loadings onto individual PCs. Two principal components (PCs) were retained for the PCA model, explaining a total of 61% of the total variance in the data. Bartlett's test was statistically significant at the 0.05 level. Element variable loading values and percentage explained by the model for the two PCs, and the communalities, i.e. the proportion of the variance of the element variables explained by the model, are presented in Table 4. The resulting biplot, which shows the PCA variable loadings and the sample scores, is shown in Fig. 1.

The first PC showed high loadings mostly for elements of largely crustal origin (Co, Sc, Th, Al, Fe, Mn, V, and Ce). EF values were low for most of these elements, indicating resuspension of crustal derived road dust as the most likely source. However, Sb, W, Cr, and Ni had higher mean EFs and are known to be associated with vehicle emissions. Ni and Sb are commonly linked to motor vehicle traffic, specifically brake pad wear [44,45], but were also associated with the presumed crustal derived elements in this study. W is emitted from studded tire wear during the winter season [46]. In the sampled winter season, roughly 30% of the cars in Trondheim used studded tires. Although overall low, W levels were indeed elevated in spring at both sampling sites, indicating contribution to W levels within the UFP fraction from vehicles using studded tires when the roads have dried.

PC2 was associated with several elements typically derived from motor vehicle emissions such as Zn, As, Sb, Rb, Pb, and Cu [40]. However, Sr and Ce which also load onto PC2 are primarily associated with crustal materials. Some elements, particularly Cs, Tl, and Sn, occurred at low concentrations within UFPs and had low PCA communalities, making source identification uncertain. Ce, Cr, and Sb showed high to intermediate loadings onto both PC1 and PC2, which indicates both vehicle traffic and crustal origins for these elements. Vehicular derived emissions indeed may deposit to the ground and mix with soil particles of crustal origin, and this road dust can eventually be re-suspended into the air, complicating urban air quality and source identification studies. According to previous studies of road dust, Fe is often associated with brake pad wear [47], in addition to Cu, Sb [48], Zn and Ni [45]. Zn [49], Cu, Sb, and Fe [44,50] are associated also with tire wear, and Zn also with exhaust emissions [40]. However, these studies did not investigate element contents within the UFP fraction specifically. The study conducted by Gugamsetty et al. [36] indicated that the percentage contribution and relative mass of elements from vehicular emissions within $PM_{0.1}$ were comparable to those within the fine size fraction, whereas soil dust contributed less for $PM_{0.1}$, as expected. Lin et al. [37] found that commonly traffic-derived metals such as Zn, Sb, and Pb typically exhibit bimodal air concentration distributions, with peaks both within the ultrafine/nano and the fine or coarse ranges.

Wood stove heating contributes significantly to urban particulate matter levels, especially in cold winter periods. However, the composition of wood stove emissions are highly variable [51], and without knowledge on the elemental composition of the local source it was not possible to estimate the relative contribution of wood stoves to UFP levels or to identify elements associated with this source.

With the exception of most winter samples and some fall samples, most samples grouped together on the PCA biplot (Fig. 1), showing that the differences between the sampling sites and seasons were small for the majority of the samples. Source apportionment using PCA provides only indications of possible sources; further studies would be needed on elemental composition of the individual possible sources to conclude. Low amounts of UFPs and associated elements, high degree of correlation between the elements in question, and individual elevated values are factors that further complicate source apportionment of elemental components using PCA.

3.6. Bioaccessibility of UFP elemental constituents

Extraction of particulate matter samples in simulated lung fluids constitutes a simple and cost-effective procedure for assessing element solubility for inhaled particles [29,52]. Element solubility in Gamble's solution reflects bioaccessibility for inhaled particles that access the interstitial lung fluid within the alveoli.

Solubility of UFP elemental components after extraction in SLFs (Gamble's solution and ALF) are shown in Table 5, and in Fig. 2a (Elgeseter) and 2b (Torget). For the elements for which solubility in Gamble's solution could be assessed, mean solubility was highest for Rb, Ni, As, Sn, Tl, and Cs (in order of decreasing solubility). Following Gamble's solution extraction, the least soluble elements were Fe and Al in Elgeseter, and Cr in Torget

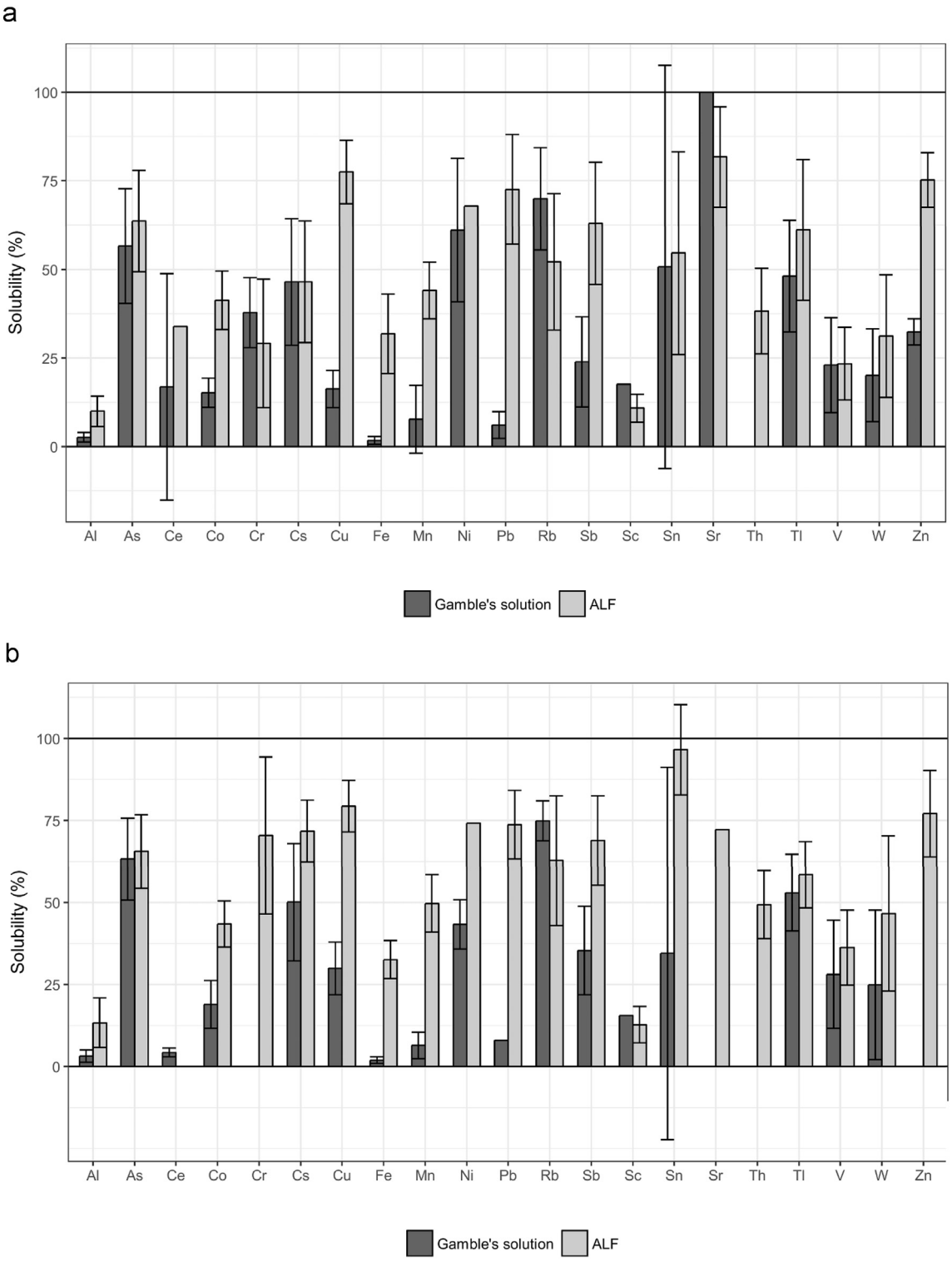

Fig. 2. Bar plots showing mean solubilities (in %) and standard deviations for elements in ultrafine particles (UFP) after extraction in the two simulated lung fluids (SLFs) Gamble's solution and artificial lysosomal fluid (ALF) for a) Elgeseter, and b) Torget samples.

samples. After extraction in ALF, Al had the lowest solubilities. These results are comparable to those found by Wiseman and Zereini [24] for As, Sb, and V in airborne PM_1 collected in a trafficked area in Frankfurt, Germany, although they reported somewhat higher overall solubility of these elements. Da Silva et al. [25] found high average solubility in Gamble's solution for Co, Fe, Mn, and V for the PM_{10} fraction from an urban area (Rio de Janeiro City, Brazil). Huang et al. [26], on the other hand, found higher solubility for Cu and Zn than for As in urban $PM_{2.5}$ collected in Singapore, whereas Coufalík et al. [27] obtained much higher solubility for V compared to Cu, Ni, and Cr in urban PM_1 fraction samples collected in Brno, Czech Republic, both studies using Gamble's solution. However, none of these studies investigated element solubility within the UFP fraction.

Solubility was overall higher in Torget compared to Elgeseter station. As expected, for most of the studied elements overall element solubilities were considerably higher after extraction in the acidic ALF, which represents

conditions in lung cells following phagocytosis of particles caused by stress reactions, than in the neutral Gamble's solution. This is in accordance with findings by Wiseman and Zereini [24].

Mean solubility varied considerably between the different elemental UFP components. The variation was also high for individual elements; for instance, Cs solubility after Gamble's solution extraction ranged from 21% to 86% in Elgeseter and from 15% to 90% in Torget samples. Extensive variability in solubility has also been observed in other studies on the bioaccessibility of APM elemental components [24,25]. In the present work the low dust amounts on the filters and the relatively low solubility after Gamble's solution extraction for most elements studied resulted in low element concentrations in the extract samples, and thereby considerable proportions of values below the LODs. Since the HNO_3 soluble and not the total element fraction was analyzed, solubilities reported in this study are most likely overestimated. Another challenge in the use of SLFs is their instability; new solutions must be made before each experiment, and pH must be checked after extraction to control for degradation [29]. In this study, pH mostly remained stable within ±0.1 pH units, indicating that degradation of the solution has not significantly affected the results. It is also important to keep in mind that element solubility in SLFs does not necessarily correspond to the actual bioavailability in individuals, which may vary considerably depending on external factors such as wind, precipitation, and distance from the road, and individual variability and contingencies with respect to inhalation, deposition, clearance, and toxicity. However, simple tests such as solubility in SLFs offer more reproducible results that can be useful in monitoring and toxicity assessment studies.

Since relatively little research has been conducted on airborne total and bioaccessible UFP concentrations and associated adverse health effects, and ambient levels typically found in urban areas seem to be associated with adverse respiratory and cardiovascular outcomes, the ultrafine fraction should receive more attention in future studies.

4. Conclusions

Total concentrations of airborne ultrafine particles (UFPs) were overall higher at the roadside Elgeseter compared to the Torget background sampling station in the city of Trondheim, Norway. UFP levels were elevated in winter (November–February) at Torget. Overall, airborne UFP and concentrations of associated elements were variable, but low at both sites. UFP concentrations of Al, Sc, and Th were elevated in spring and summer at Elgeseter, indicating re-suspension by vehicles of road dust containing both road traffic dust and natural soils. W levels were considerably higher in spring, most probably originating from asphalt wear by studded tires.

Source identification investigation with principal component analysis (PCA) indicated that the two predominant sources of elements in UFPs were material originating from the Earth's crust, and road traffic emissions. Elements most clearly associated with vehicular traffic were: Zn, Rb, Sb, Pb, As, and Cu. Several elements, including Sb, Cr, and Ce, seemed to originate both from road traffic and natural soils. Enrichment factor analysis confirmed that the following elements associated with UFPs most probably originated predominantly from anthropogenic sources, listed in order of decreasing EF: Sb > Sn > As > Zn > Pb > Cu. W and Tl also were probably mainly of anthropogenic origin.

This is the first study investigating bioaccessibility of elements in the ultrafine particulate fraction. Bioaccessibility investigation using simulated lung fluids showed relatively high solubilities in Gamble's solution for the following UFP-associated elements: Rb, Ni, As, Sn, Tl, and Cs, whereas Fe, Al, and Cr had the overall lowest solubilities. For most of the studied elements, solubility was generally somewhat higher in Torget compared to Elgeseter samples. Element solubility was for the most part considerably higher after extraction in the more acidic artificial lysosomal fluid (ALF) compared to the neutral Gamble's solution.

Declaration of Competing Interest

The authors declare that they have no known competing financial interests or personal relationships that could have appeared to influence the work reported in this paper.

Acknowledgements

The project was partially funded by the Norwegian foundation “Anders Jahres fond til vitenskapens fremme”. We thank the Norwegian Public Roads Administration (NPRA) and Trondheim Municipality for permission to use Elgeseter and Torget measurement stations, and for assistance in installing the equipment. We also thank Zahra Galal Mahmud for assistance in collecting samples and laboratory analysis work, and Syverin Lierhagen for conducting HR-ICP-MS analyses and for general assistance and supervision with laboratory work.

Appendix A. Supplementary data

Supplementary data to this article can be found online at https://doi.org/10.1016/j.enceco.2019.08.001.

References

[1] P.J. Landrigan, R. Fuller, N.J.R. Acosta, O. Adeyi, R. Arnold, N.N. Basu, et al., The Lancet Commission on pollution and health, Lancet 391 (2018) 462–512, https://doi.org/10.1016/S0140-6736(17)32345-0.
[2] World Health Organization (WHO) Europe, Air Quality Guidelines Global Update 2005 Particulate Matter, Ozone, Nitrogen Dioxide and Sulfur Dioxide, Germany 2006.
[3] K.T. Whitby, W.E. Clark, V.A. Marple, G.M. Sverdrup, G.J. Sem, K. Willeke, et al., Characterization of California aerosols—I. Size distributions of freeway aerosol, Atmos. Environ. 9 (1975) 463–482, https://doi.org/10.1016/0004-6981(75)90107-9.
[4] J. Hitchins, L. Morawska, R. Wolff, D. Gilbert, Concentrations of submicrometre particles from vehicle emissions near a major road, Atmos. Environ. 34 (2000) 51–59, https://doi.org/10.1016/S1352-2310(99)00304-0.
[5] Y. Zhu, W.C. Hinds, S. Kim, C. Sioutas, Concentration and size distribution of ultrafine particles near a major highway, J. Air Waste Manag. Assoc. 52 (2002) 1032–1042.
[6] J. Pekkanen, A. Peters, G. Hoek, P. Tiittanen, B. Brunekreef, J. de Hartog, et al., Particulate air pollution and risk of ST-segment depression during repeated submaximal exercise tests among subjects with coronary heart disease: the exposure and risk assessment for fine and ultrafine particles in ambient air (ULTRA) study, Circulation 106 (2002) 933–938.
[7] A. Peters, H.E. Wichmann, T. Tuch, J. Heinrich, J. Heyder, Respiratory effects are associated with the number of ultrafine particles, Am. J. Respir. Crit. Care Med. 155 (1997) 1376–1383, https://doi.org/10.1164/ajrccm.155.4.9105082.
[8] M. Stölzel, A. Peters, J. Cyrys, M. Pitz, G. Wölke, W. Kreyling, et al., Particulate matter in several size classes and daily mortality in Erfurt, Germany, Epidemiology 15 (2004) S59.
[9] H.E. Wichmann, C. Spix, T. Tuch, G. Wölke, A. Peters, J. Heinrich, et al., Daily mortality and fine and ultrafine particles in Erfurt, Germany part I: role of particle number and particle mass, Res Rep Health Eff Inst Report No. 86, 2000.
[10] D.M. Brown, V. Stone, P. Findlay, W. MacNee, K. Donaldson, Increased inflammation and intracellular calcium caused by ultrafine carbon black is independent of transition metals or other soluble components, Occup. Environ. Med. 57 (2000) 685–691.
[11] G. Oberdörster, Z. Sharp, V. Atudorei, A. Elder, R. Gelein, W. Kreyling, et al., Translocation of inhaled ultrafine particles to the brain, Inhal. Toxicol. 16 (2004) 437–445, https://doi.org/10.1080/08958370490439597.
[12] J.S. Brown, K.L. Zeman, W.D. Bennett, Ultrafine particle deposition and clearance in the healthy and obstructed lung, Am. J. Respir. Crit. Care Med. 166 (2002) 1240–1247, https://doi.org/10.1164/rccm.200205-399OC.
[13] M. Geiser, B. Rothen-Rutishauser, N. Kapp, S. Schürch, W. Kreyling, H. Schulz, et al., Ultrafine particles cross cellular membranes by nonphagocytic mechanisms in lungs and in cultured cells, Environ. Health Perspect. 113 (2005) 1555–1560, https://doi.org/10.1289/EHP.8006.
[14] M. Franklin, P. Koutrakis, P. Schwartz, The role of particle composition on the association between PM2.5 and mortality, Epidemiology 19 (2008) 680–689.
[15] R.T. Burnett, J. Brook, T. Dann, C. Delocla, O. Philips, S. Cakmak, et al., Association between particulate- and gas-phase components of urban air pollution and daily mortality in eight Canadian cities, Inhal. Toxicol. 12 (2000) 15–39, https://doi.org/10.1080/08958370050164851.
[16] M.L. Bell, K. Ebisu, R.D. Peng, J.M. Samet, F. Dominici, Hospital admissions and chemical composition of fine particle air pollution, Am. J. Respir. Crit. Care Med. 179 (2009) 1115–1120, https://doi.org/10.1164/rccm.200808-1240OC.
[17] M.M. Patel, L. Hoepner, R. Garfinkel, S. Chillrud, A. Reyes, J.W. Quinn, et al., Ambient metals, elemental carbon, and wheeze and cough in New York City children through 24 months of age, Am. J. Respir. Crit. Care Med. 180 (2009) 1107–1113, https://doi.org/10.1164/rccm.200901-0122OC.

[18] D.L. Costa, K.L. Dreher, Bioavailable transition metals in particulate matter mediate cardiopulmonary injury in healthy and compromised animal models, Environ. Health Perspect. 105 (Suppl. 5) (1997) 1053–1060.
[19] A.J. Ghio, C. Kim, R.B. Devlin, Concentrated ambient air particles induce mild pulmonary inflammation in healthy human volunteers, Am. J. Respir. Crit. Care Med. 162 (2000) 981–988, https://doi.org/10.1164/ajrccm.162.3.9911115.
[20] M. Valko, K. Jomova, C.J. Rhodes, K. Kuča, K. Musílek, Redox- and non-redox-metal-induced formation of free radicals and their role in human disease, Arch. Toxicol. 90 (2016) 1–37, https://doi.org/10.1007/s00204-015-1579-5.
[21] J.D. McNeilly, M.R. Heal, I.J. Beverland, A. Howe, M.D. Gibson, L.R. Hibbs, et al., Soluble transition metals cause the pro-inflammatory effects of welding fumes in vitro, Toxicol. Appl. Pharmacol. 196 (2004) 95–107, https://doi.org/10.1016/j.taap.2003.11.021.
[22] C. Colombo, A.J. Monhemius, J.A. Plant, Platinum, palladium and rhodium release from vehicle exhaust catalysts and road dust exposed to simulated lung fluids, Ecotoxicol. Environ. Saf. 71 (2008) 722–730, https://doi.org/10.1016/j.ecoenv.2007.11.011.
[23] F. Zereini, C.L.S. Wiseman, W. Püttmann, In vitro investigations of platinum, palladium, and rhodium mobility in urban airborne particulate matter (PM10, PM2.5, and PM1) using simulated lung fluids, Environ. Sci. Technol. 46 (2012) 10326–10333, https://doi.org/10.1021/es3020887.
[24] C.L.S. Wiseman, F. Zereini, Characterizing metal(loid) solubility in airborne PM10, PM2.5 and PM1 in Frankfurt, Germany using simulated lung fluids, Atmos. Environ. 89 (2014) 282–289, https://doi.org/10.1016/J.ATMOSENV.2014.02.055.
[25] L.I.D. da Silva, L. Yokoyama, L.B. Maia, M.I.C. Monteiro, F.V.M. Pontes, M.C. Carneiro, et al., Evaluation of bioaccessible heavy metal fractions in PM10 from the metropolitan region of Rio de Janeiro city, Brazil, using a simulated lung fluid, Microchem. J. 118 (2015) 266–271, https://doi.org/10.1016/j.microc.2014.08.004.
[26] X. Huang, R. Betha, L.Y. Tan, R. Balasubramanian, Risk assessment of bioaccessible trace elements in smoke haze aerosols versus urban aerosols using simulated lung fluids, Atmos. Environ. 125 (2016) 505–511, https://doi.org/10.1016/J.ATMOSENV.2015.06.034.
[27] P. Coufalík, P. Mikuška, T. Matoušek, Z. Večeřa, Determination of the bioaccessible fraction of metals in urban aerosol using simulated lung fluids, Atmos. Environ. 140 (2016) 469–475, https://doi.org/10.1016/J.ATMOSENV.2016.06.031.
[28] European Committee for Standardization (CEN). EN 12341, Ambient Air - Standard Gravimetric Measurement Method for the Determination of the PM10 or PM2,5 Mass Concentration of Suspended Particulate Matter 2014, https://standards.cen.eu/dyn/www/f?p=204:110:0::::FSP_PROJECT,FSP_ORG_ID:29133,6245&cs=1DC6EB16DD302E384B46A7097AAC67CB5 2014, Accessed date: 7 November 2017.
[29] G. Herting, I. Odnevall Wallinder, C. Leygraf, Metal release from various grades of stainless steel exposed to synthetic body fluids, Corros. Sci. 49 (2007) 103–111, https://doi.org/10.1016/j.corsci.2006.05.008.
[30] O.R. Moss, Simulants of lung interstitial fluid, Health Phys. 36 (1979) 447–448.
[31] W. Stopford, J. Turner, D. Cappellini, T. Brock, Bioaccessibility testing of cobalt compounds, J. Environ. Monit. 5 (2003) 675–680.
[32] M.R. Flynn, Analysis of censored exposure data by constrained maximization of the Shapiro–Wilk W statistic, Ann. Occup. Hyg. 54 (2010) 263–271, https://doi.org/10.1093/annhyg/mep083.
[33] W.H. Zoller, E.S. Gladney, R.A. Duce, Atmospheric concentrations and sources of trace metals at the south pole, Science 183 (1974) 198–200, https://doi.org/10.1126/science.183.4121.198.
[34] B. Mason, C.B. Moore, Principles of Geochemistry, 4th ed. John Wiley & Sons, 1982.
[35] T.A. Pakkanen, V.-M. Kerminen, C.H. Korhonen, R.E. Hillamo, P. Aarnio, T. Koskentalo, et al., Urban and rural ultrafine (PM0.1) particles in the Helsinki area, Atmos. Environ. 35 (2001) 4593–4607, https://doi.org/10.1016/S1352-2310(01)00167-4.
[36] B. Gugamsetty, H. Wei, C.-N. Liu, A. Awasthi, S.-C. Hsu, C.-J. Tsai, et al., Source characterization and apportionment of PM 10, PM 2.5 and PM 0.1 by using positive matrix factorization, Aerosol Air Qual. Res. 12 (2012) 476–491, https://doi.org/10.4209/aaqr.2012.04.0084.
[37] C.-C. Lin, S.-J. Chen, K.-L. Huang, W.-I. Hwang, G.-P. Chang-Chien, W.-Y. Lin, Characteristics of metals in nano/ultrafine/fine/coarse particles collected beside a heavily trafficked road, Environ. Sci. Technol. 39 (2005) 8113–8122.
[38] D.S. Lee, J.A. Garland, A.A. Fox, Atmospheric concentrations of trace elements in urban areas of the United Kingdom, Atmos. Environ. 28 (1994) 2691–2713, https://doi.org/10.1016/1352-2310(94)90442-1.
[39] R.C. Ragaini, H.R. Ralston, N. Roberts, Environmental trace metal contamination in Kellogg, Idaho, near a lead smelting complex, Environ. Sci. Technol. 11 (1977) 773–781, https://doi.org/10.1021/es60131a004.
[40] F. Amato, M. Pandolfi, M. Viana, X. Querol, A. Alastuey, T. Moreno, Spatial and chemical patterns of PM 10 in road dust deposited in urban environment, Atmos. Environ. 43 (2009) 1650–1659, https://doi.org/10.1016/j.atmosenv.2008.12.009.
[41] J. Asheim, K. Vike-Jonas, S.V. Gonzalez, S. Lierhagen, V. Venkatraman, I.-L.S. Veivåg, et al., Benzotriazoles, benzothiazoles and trace elements in an urban road setting in Trondheim, Norway: re-visiting the chemical markers of traffic pollution, Sci. Total Environ. 649 (2019) 703–711, https://doi.org/10.1016/J.SCITOTENV.2018.08.299.
[42] R.A. Duce, G.L. Hoffman, W.H. Zoller, Atmospheric trace metals at remote northern and southern hemisphere sites: pollution or natural? Science 187 (1975) 59–61, https://doi.org/10.1126/science.187.4171.59.
[43] C. Reimann, P. de Caritat, Intrinsic flaws of element enrichment factors (EFs) in environmental geochemistry, Environ. Sci. Technol. 34 (2000) 5084–5091, https://doi.org/10.1021/es001339o.
[44] A. Thorpe, R.M. Harrison, Sources and properties of non-exhaust particulate matter from road traffic: a review, Sci. Total Environ. 400 (2008) 270–282, https://doi.org/10.1016/j.scitotenv.2008.06.007.
[45] F. Amato, X. Querol, C. Johansson, C. Nagl, A. Alastuey, A review on the effectiveness of street sweeping, washing and dust suppressants as urban PM control methods, Sci. Total Environ. 408 (2010) 3070–3084, https://doi.org/10.1016/j.scitotenv.2010.04.025.
[46] M. Bäckström, U. Nilsson, K. Håkansson, B. Allard, S. Karlsson, Speciation of heavy metals in road runoff and roadside total deposition, Water Air Soil Pollut. 147 (2003) 343–366, https://doi.org/10.1023/A:1024545916834.
[47] J.J. Schauer, G.C. Lough, M.M. Shafer, W.F. Christensen, M.F. Arndt, J.T. DeMinter, et al., Characterization of metals emitted from motor vehicles, Res. Rep. Health Eff. Inst. (2006) 1–76 (discussion 77-88).
[48] J. Sternbeck, Å. Sjödin, K. Andréasson, Metal emissions from road traffic and the influence of resuspension—results from two tunnel studies, Atmos. Environ. 36 (2002) 4735–4744, https://doi.org/10.1016/S1352-2310(02)00561-7.
[49] G. Weckwerth, Verification of traffic emitted aerosol components in the ambient air of Cologne (Germany), Atmos. Environ. 35 (2001) 5525–5536, https://doi.org/10.1016/S1352-2310(01)00234-5.
[50] K. Adachi, Y. Tainosho, Characterization of heavy metal particles embedded in tire dust, Environ. Int. 30 (2004) 1009–1017, https://doi.org/10.1016/j.envint.2004.04.004.
[51] C. Schmidl, I.L. Marr, A. Caseiro, P. Kotianova, A. Berner, H. Bauer, et al., Chemical characterisation of fine particle emissions from wood stove combustion of common woods growing in mid-European Alpine regions, Atmos. Environ. 42 (2008) 126–141, https://doi.org/10.1016/J.ATMOSENV.2007.09.028.
[52] A. Mukhtar, A. Limbeck, Recent developments in assessment of bio-accessible trace metal fractions in airborne particulate matter: a review, Anal. Chim. Acta 774 (2013) 11–25, https://doi.org/10.1016/j.aca.2013.02.008.